JOURNAL OF Materials Communication CHEMISTRY

The effect of large magnetic fields on solid state combustion reactions: novel microstructure, lattice contraction and reduced coercivity in barium hexaferrite

Marco D. Aguas,[a] Louise Affleck,[a,b] Ivan P. Parkin,[a] Maxim V. Kuznetsov,[b] W. Andrew Steer,*[b] Quentin A. Pankhurst,*[b] Luis Fernández Barquín,[c] Mark A. Roberts,[d] Marius I. Boamfa[e] and Jos A. A. J. Perenboom[e]

[a]*Department of Chemistry, University College London, 20 Gordon Street, London, UK WC1H 0AJ*
[b]*Department of Physics and Astronomy, University College London, Gower Street, London, UK WC1E 6BT. E-mail: q.pankhurst@ucl.ac.uk*
[c]*Departamento CITIMAC, Facultad de Ciencias, Universidad de Cantabria, Santander 39005, Spain*
[d]*CLRC Daresbury Laboratory, Warrington, Cheshire, UK WA4 4AD*
[e]*Research Institute for Materials and High Field Magnet Laboratory, University of Nijmegen, 6525 ED Nijmegen, The Netherlands*

Received 16th November 1999, Accepted 24th November 1999

Combustion reactions of BaO_2, Fe_2O_3 and Fe performed in large applied fields have revealed unexpected modifications in the microstructure of the multiphase combustion product, and in the lattice parameters and coercivity of monophase $BaFe_{12}O_{19}$ obtained by post-production grinding and sintering.

To date there has been limited research into the effects of applied magnetic fields on combustion processes. Most reports deal with gaseous combustion. It has been shown that a field gradient can promote gas phase combustion *via* the action of a magnetic force on paramagnetic oxygen molecules, leading to convection and improved air flow to the flame front.[1–3] Similarly, it has been proposed that a uniform field can modify the flow of ionised gases in solid rocket motors, thereby affecting the static pressure and the rate of combustion.[4] Meanwhile, the possible influence of an applied magnetic field on solid state combustion has been largely overlooked, despite the growing recognition of the technological importance of such processing routes.[5,6]

Self-propagating high-temperature synthesis (SHS) reactions are driven by their reaction enthalpy.[5] They can be initiated by a hot wire and proceed *via* a propagation wave through a ceramic powder or compact, generating fast heating (up to 1200 °C in less than a second) and rapid cooling. Until recently the only reported results for SHS reactions in an external field were the observation of increased reaction rate and temperature in titanium carbide[7] and strontium hexaferrite.[8] However, in the last few years we have conducted studies of the effect of applied fields (up to 1.1 T) on both the post-SHS products and the subsequently ground and sintered end-products of several hard and soft magnetic materials.[9–12] In all cases both the temperature and velocity of the solid flame propagation wave increased in the applied field. Changes were seen in the bulk magnetic properties of the ground and sintered end-products, such as a 20% decrease in coercivity in $BaFe_{12}O_{19}$,[11] and magnetisation increases of 15% in $MgFe_2O_4$ and 35% in $Mg_{0.5}Zn_{0.5}Fe_2O_4$.[10] Incorporating other elements into the samples could modify these differences, *e.g.* the coercivity change rose to almost 100% for $BaFe_{10}Cr_2O_{19}$.[11] These are significant effects, with potential for exploitation in the world-wide ferrite magnet industry. However, a lack of understanding of how the applied fields influenced the solid state combustion was a barrier to further work. In response to this, we undertook experiments at the Nijmegen High Field Magnet Laboratory in which SHS reactions were subjected to fields of up to 15 T. The use of such large fields accentuated the effect of the field on the combustion process, with unexpected results.

Reactions were carried out under a flow of oxygen gas (10 l min^{-1}) on 17 mm diameter disks of 1 g aliquots from a 35 g mixture of iron, iron oxide and barium peroxide powders, pressed to 88 MPa. The disks were supported by a quartz glass tripod inside a 30 mm inner diameter quartz tube in the centre of a 20 T Bitter magnet. The reactions were initiated using a nichrome wire hot filament on a small charge of titanium in silicon-grease paste on the edge of the disk. The reaction conditions (gas flow rate, period of time the magnet was switched on, positioning of sample, placement of the hot filament ignitor) were identical for all the reactions, so that the field was the only variable. The idealised reaction equation was:

$$BaO_2 + 6Fe + 3Fe_2O_3 + 4O_2 \rightarrow BaFe_{12}O_{19} \quad (1)$$

Reactions were performed at zero field and in applied fields of 5, 10 and 15 T. On inspection it was clear that the reactions increased in both speed and evolved heat as the field was increased. The synthesis wave velocity and temperature were independently estimated (by optical pyrometry) to be *ca.* 5 mm s^{-1} and 1050 °C in a field of 1.1 T, and 2 mm s^{-1} and 975 °C in zero field. Post-SHS sintering was performed on powder products in open ceramic boats in a rapid heating furnace (heating and cooling at 20 °C min^{-1}, maximum 1200 °C for 2 h). The post-SHS and post-sintering samples were characterised by SEM/EDAX, electron microprobe analysis (using a 1 μm^2 beam), high resolution X-ray diffraction data ($\lambda = 0.6920$ Å, on a curved image plate detector at Daresbury Laboratory, UK[13]), bulk magnetometry (in fields up to 5 kOe) and ^{57}Fe Mössbauer spectroscopy.

Unexpectedly, the applied field SHS products all showed two macroscopically distinct parts, one metallic in appearance, and the other non-metallic in appearance (see Fig. 1). SEM/EDAX showed that the overall Ba and Fe composition was in keeping with the reagent amounts, and indicated different granular microstructures in the post-SHS metallic and non-metallic phases. More detailed electron microprobe data showed that *ca.* 50% of the metallic phase samples had acicular microstructures, as shown in Fig. 2. Grains of order 100–300 μm long by 10–20 μm wide were present, along with more homogeneous

Fig. 1 Photograph of the product of an SHS reaction of SrO_2, Fe and Fe_2O_3 in an applied field of 15 T. The disk has a diameter of 17 mm. The clear separation between metallic and non-metallic parts is typical of the products of hexaferrite reactions.

regions characterised by crystallites of order 1 μm in size. Spot analysis showed that the acicular grains had Ba : Fe in a 1 : 12 ratio, surrounded by a relatively Ba-rich phase in which the Ba : Fe ratio was close to 1 : 2. The formation of the acicular grains is consistent with there being enhanced combustion conditions in the applied field reactions, with the higher temperatures attained leading to higher diffusion rates and more rapid grain growth.

XRD data showed clear differences between the metallic and non-metallic parts (Fig. 3). Identified phases in the non-metallic part were (in order of prominence) α-Fe, α-Fe_2O_3, $BaFe_2O_4$, Fe_3O_4 and $Fe_{1-x}O$, while the phases seen in the metallic part aliquots were Fe_3O_4, $BaFe_2O_4$ and α-Fe_2O_3. (The Mössbauer effect data were in keeping with this, unambiguously identifying α-Fe, α-Fe_2O_3 and $Fe_{1-x}O$ in the non-metallic part, and having subspectra consistent with $BaFe_2O_4$ and Fe_3O_4 in all the post-SHS samples.) Given the likelihood that the α-Fe and α−Fe_2O_3 were unreacted reagents this shows that the metallic parts of the product are more fully combusted than the non-metallic parts. The absence of the end product $BaFe_{12}O_{19}$ phase in the metallic part implies that the acicular grains (which had Ba : Fe in a 1 : 12 ratio) comprise magnetite-rich fine scale mixtures of $BaFe_2O_4$ and Fe_3O_4. Furthermore,

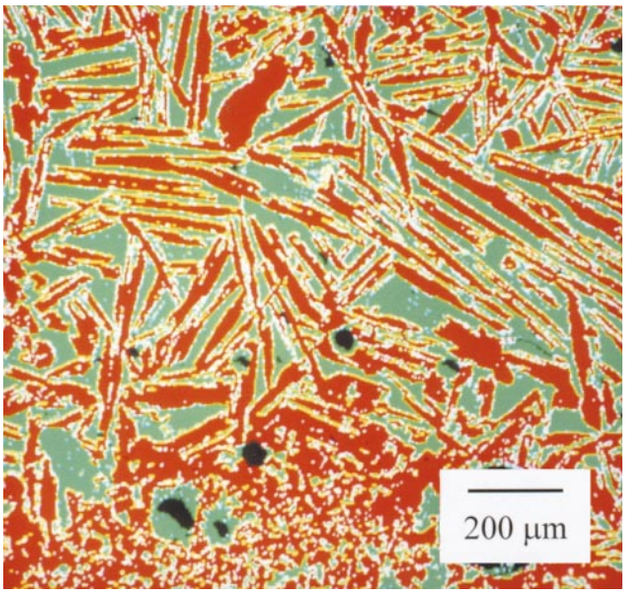

Fig. 2 Electron microprobe plot for a surface section of the metallic part of the 5 T post-SHS product. The acicular grains are Fe-rich, while the intervening material has a relatively high proportion of Ba. The black regions correspond to voids in the sample.

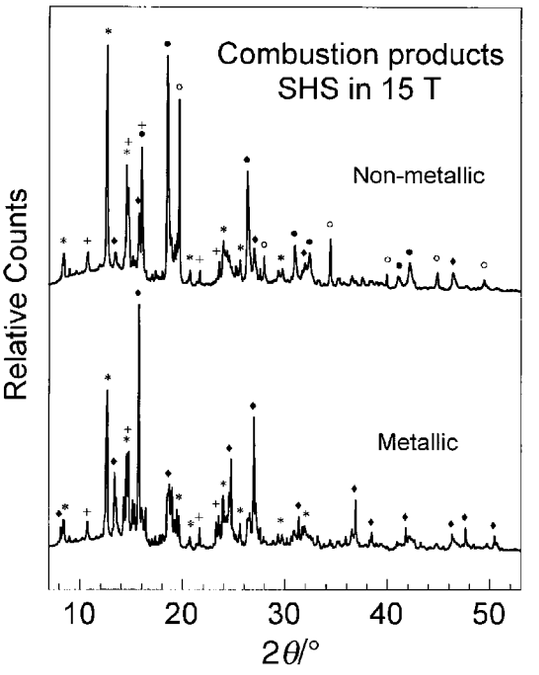

Fig. 3 X-Ray diffraction data ($\lambda = 0.6920$ Å) for the metallic and non-metallic parts of the 15 T post-SHS product. A number of phases are identified, including magnetite Fe_3O_4 (◆), α–Fe (○), α–Fe_2O_3 (+), wüstite $Fe_{1-x}O$ (●) and $BaFe_2O_4$ (*).

we can infer from the X-ray data that the reaction proceeds *via* intermediate phases. In the well combusted (metallic) regions the $BaO_2 + Fe + Fe_2O_3$ green mixture transforms to $BaFe_2O_4 + Fe_3O_4$. In the less well combusted (non-metallic) regions the product comprises $BaFe_2O_4 + [Fe + Fe_2O_3 + Fe_{1-x}O] + Fe_3O_4$, where it is plausible that the phases in square brackets are intermediaries in the route towards the formation of magnetite.

The post-sintering products were all virtually monophase $BaFe_{12}O_{19}$ as determined by XRD and Mössbauer spectroscopy. Rudimentary Rietveld analysis was performed to determine the lattice parameters *a* and *c* as a function of the

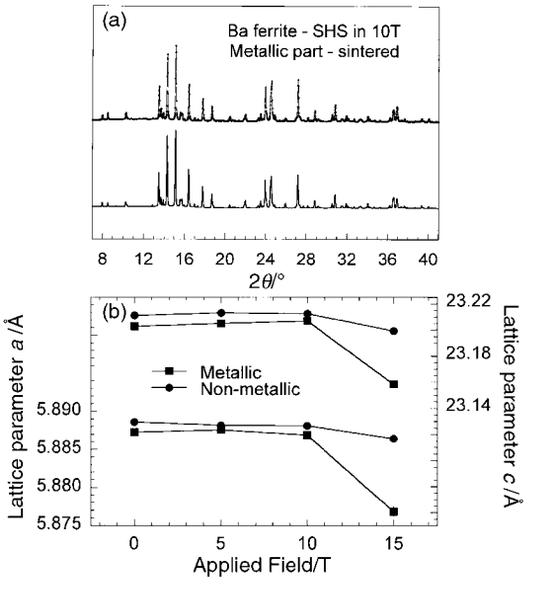

Fig. 4 (a) Representative post-sintering X-ray data ($\lambda = 0.6920$ Å) showing the close correlation between the observed diffraction peaks and those predicted for monophase $BaFe_{12}O_{19}$ (lower trace). (b) Fitted lattice parameters *a* and *c* of the post-sintering $BaFe_{12}O_{19}$ as a function of the field applied during synthesis. Error bars are given on all points, although in most cases they are smaller than the symbols used.

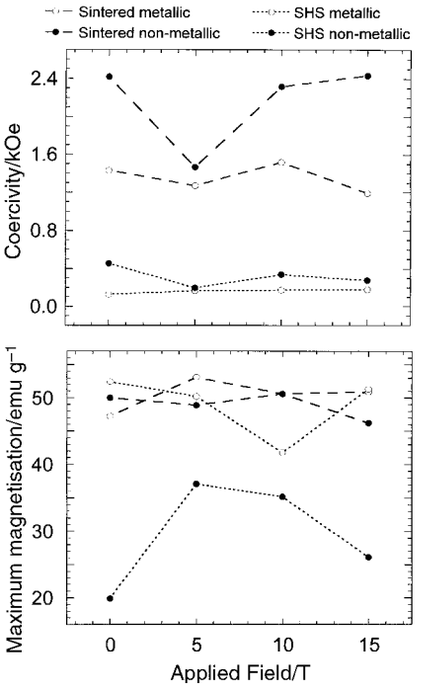

Fig. 5 Coercivity (H_c) and maximum magnetisation (σ_{max}) of the metallic and non-metallic post-SHS and post-sintering products as a function of the field applied during synthesis.

field applied during SHS (Fig. 4). A clear fall in lattice parameter appears in the 15 T samples, of a magnitude far in excess of the uncertainty in the fitted parameters. (Additional XRD runs on different sample aliquots show this result to be reproducible.) The corresponding change in unit cell volume for the latter is a reduction of order 0.5%. The origin of this structural change might be an oxygen vacancy ordering effect in the post-SHS magnetite phase, carried over into the post-sintering product. Further experiments and analysis are needed to test this hypothesis.

The observed magnetic properties of the samples (coercivity H_c and maximum magnetisation σ_{max}, Fig. 5) can be related to their different phase compositions and microstructures. In the post-SHS samples, the low H_c and high σ_{max} of the metallic part are consistent with the presence of large grain multi-domain magnetite, while the low H_c and σ_{max} of the non-metallic part reflect the influence of the relatively low magnetisation phases α-Fe_2O_3 and $Fe_{1-x}O$. The post-sintering $BaFe_{12}O_{19}$ samples show some quite marked variations in H_c. The likely reason for this is that the finer microstructures of the non-metallic post-SHS products promote a smaller grain size in the post-sintering $BaFe_{12}O_{19}$, with a larger H_c then corresponding to more monodomain-like magnetic behaviour.

In summary, SHS reactions of BaO_2, Fe_2O_3 and Fe in applied fields of up to 15 T have provided new insights into field-assisted combustion processes. The products comprise two distinct parts, metallic and non-metallic in appearance, with the former associated with enhanced combustion and rapid grain growth of magnetite-rich phases. The lattice parameters and coercivities of monophase $BaFe_{12}O_{19}$ samples obtained by subsequent grinding and heating of the combustion products are different for the metallic and non-metallic parts, and depend on the magnitude of the field applied during combustion. This result establishes the use of applied field in solid state combustion syntheses as a new route to the modification and control of the structural, microstructural and magnetic properties of ferrite magnets.

Acknowledgements

We thank the Royal Society for support *via* their FSU Programme, the British Council and the Spanish CICYT for support *via* an Acciones Integradas collaborative grant, and the European Union for enabling access to the high magnetic fields under contract CT950079. The Mössbauer data were collected *via* the University of London Intercollegiate Research Service.

References

1 N. I. Wakayama, *Chem. Phys. Lett.*, 1992, **188**, 279.
2 N. I. Wakayama, *Combust. Flame*, 1993, **93**, 207.
3 N. I. Wakayama, *J. Jpn. Inst. Metals*, 1997, **61**, 1272.
4 I. G. Borovskoi and A. B. Vorozhtsov, *J. Propulsion Power*, 1995, **11**, 824.
5 H. C. Yi and J. J. Moore, *J. Mater. Sci.*, 1990, **25**, 1159.
6 A. G. Merzhanov, *Int. J. Self-Propag. High-Temp. Synth.*, 1997, **6**, 119.
7 A. I. Kirdyashkin, Y. M. Maksimov and A. G. Merzhanov, *Combust. Explos. Shock Waves*, 1986, **22**, 700.
8 A. V. Komarov, Y. G. Morozov, P. B. Avakyan and M. D. Nersesyan, *Int. J. Self-Propag. High-Temp. Synth.*, 1994, **3**, 207.
9 M. V. Kuznetsov, Q. A. Pankhurst and I. P. Parkin, *J. Phys. D*, 1998, **31**, 2886.
10 M. V. Kuznetsov, Q. A. Pankhurst and I. P. Parkin, *J. Mater. Chem.*, 1998, **8**, 2701.
11 I. P. Parkin, M. V. Kuznetsov and Q. A. Pankhurst, *J. Mater. Chem.*, 1999, **9**, 273.
12 W. B. Cross, L. Affleck, M. V. Kuznetsov, I. P. Parkin and Q. A. Pankhurst, *J. Mater. Chem.*, 1999, **9**, 2545.
13 M. A. Roberts, J. L. Finney and G. Bushnell-Wye, *Mater. Sci. Forum*, 1998, **278–281**, 318.

Communication a909062b